Am J Cancer Res 2022;12(11):5049-5061
www.ajcr.us /ISSN:2156-6976/ajcr0146842

Original Article

Combination treatment of arsenic trioxide and osimertinib in recurrent and metastatic head and neck squamous cell carcinoma

Ching-Yun Hsieh[1*], Wei-Chao Chang[2*], Ching-Chan Lin[1], Jong-Hang Chen[1], Chen-Yuan Lin[1], Chia-Hua Liu[1], Chen Lin[2], Mien-Chie Hung[2,3,4,5]

[1]Division of Hematology and Oncology, Department of Internal Medicine, China Medical University Hospital, China Medical University, Taichung 40402, Taiwan; [2]Center for Molecular Medicine, China Medical University Hospital, China Medical University, Taichung 40402, Taiwan; [3]Research Center for Cancer Biology, China Medical University, Taichung 40402, Taiwan; [4]College of Medicine, Graduate Institute of Biomedical Sciences, China Medical University, Taichung 40402, Taiwan; [5]Department of Biotechnology, Asia University, Taichung 40402, Taiwan. [*]Equal contributors.

Received October 5, 2022; Accepted October 30, 2022; Epub November 15, 2022; Published November 30, 2022

Abstract: Recurrent and/or metastatic (R/M) head and neck squamous cell carcinoma (HNSCC) represents an advanced stage of the disease and frequently shows resistance to these current treatments, including platinum chemotherapy, cetuximab plus chemotherapy, and checkpoint inhibitors. EGFR overexpression and *TP53* mutation are the most frequent genetic changes in patients with HNSCC. On the basis of this genetic feature, we proposed a combinatorial treatment using the EGFR tyrosine kinase inhibitor osimertinib (AZD) and arsenic trioxide (ATO) for compassionate use. The patient obtained treatment response and progression-free survival for about six months. *In vitro* mechanical verifications showed that ATO and AZD combination (ATO/AZD) significantly increased intracellular ROS levels and DNA damage. Additionally, ATO/AZD decreases the expression and activity of breast cancer type 1 susceptibility protein (BRCA1) and polo-like kinase 1 (PLK1), thereby impairing Rad51 recruitment to DNA double-strand lesion for repair and may ultimately cause tumor cell death. In conclusion, this study provides a concrete experience and an alternate strategy of ATO/AZD therapy for patients with R/M HNSCC.

Keywords: Head and neck squamous cell carcinoma, arsenic trioxide, osimertinib, DNA damage response

Introduction

Head and neck squamous cell carcinoma (HNSCC), developing in the outer layer of skin and the mucous membranes of the mouth, nose, and throat, is the seventh most common cancer type worldwide, accounting for about 900,000 new cases annually [1]. Because of the lack of effective screening strategies for early detection, most patients are diagnosed at an advanced stage of the disease with a 5-year overall survival rate of less than 50% [2]. Surgical resection is the priority treatment for HNSCC of the oral cavity [3]. Radiotherapy (RT) or chemotherapy (CT) combined with RT (chemoradiotherapy; CRT) are considered in patients with unresectable tumors or serve as adjuvant treatments to lower high-risk characteristics of patients [4]. Additionally, CRT is the primary treatment for patients having pharyngeal and laryngeal cancers. The combination of cisplatin and 5-fluorouracil (PF) is a frequently used chemotherapeutic HNSCC regimen [5]. The addition of docetaxel to PF (TPF) currently offers a revolutionary treatment strategy that shows an advantage in improving patient outcomes [6, 7]. Cetuximab, a chimeric monoclonal antibody of epidermal growth factor receptor (EGFR), is approved by the United States Food and Drug Administration (FDA) as an RT sensitizer for treating of cisplatin-ineligible patients or patients with recurrent and/or metastatic (R/M) disease [8]. Recent clinical evidence from immunotherapy trials exhibited promising outcomes for the long-term survival of patients. Consequently, the immune check-

point inhibitors pembrolizumab and nivolumab are approved by the FDA to treat cisplatin-refractory R/M HNSCC; moreover, pembrolizumab is recommended as first-line therapy in patients with unresectable or metastatic disease [9-11].

Genetic instability has been identified at each stage of progression in HNSCC [12]. The changes in the molecular profiles can serve as biomarkers to predict tumor progression and response to therapeutic agents and guide treatment to improve clinical outcomes [13]. EGFR, the most frequently altered protein, is overexpressed in 80%-90% of HNSCC tumors [14]. EGFR plays an essential role in carcinogenesis and tumor evolution and is associated with poor overall survival (OS) and progression-free survival (PFS) of patients with HNSCC [15]. Cetuximab remains the only FDA-approved targeted agent for suppressing EGFR signaling in HNSCC; however, the overall response rate (ORR) to single agent is merely 10%-13% [16]. One potential mechanism for inducing low ORR of cetuximab could be because of the arginine-methylation of EGFR [17, 18]. Overexpression of other receptor tyrosine kinases, such as human epidermal growth factor receptor 2 (HER2) and tyrosine-protein kinase Met (MET), may enhance HNSCC resistance to EGFR-targeting agents [19, 20]. *TP53* is a tumor suppressor gene encoding a transcription factor p53 with functions in sustaining genomic stability, cell cycle, DNA repair, and apoptosis [21]. *TP53* is the most frequently mutated gene (more than 70%) in HNSCC tumors, particularly in the human papillomavirus (HPV)-negative subtype [22]. *TP53* mutations cause either loss of the wild-type p53 functions, or gain of tumor-promoting functions, such as increased proliferation, invasion, metastasis, and genomic instability [23], and are associated with poor OS, therapeutic resistance, and increased rate of recurrence [22]. Multiple p53-targeting vaccination strategies have been attempted. However, present p53 vaccines do not improve patient survival to justify even a phase III trial [24]. The p53 has also been shown to switch tumor suppressive function into oncogenic activity by changing the binding partner [25]. A recent study revealed that arsenic trioxide (ATO), an FDA-approved drug for acute promyelocytic leukemia, can stabilize structural p53 mutants and restore p53 function [26]. The therapeutic safety and value are currently under evaluation (Phase I trial PANDA-T0; NCT03855371).

Here, a case of a man with R/M HNSCC was presented harboring *TP53* mutation treated with the combination of EGFR tyrosine kinase inhibitor (TKI) osimertinib (AZD9291; hereafter AZD) and ATO for compassionate use. The duration of response to the treatment lasted for 24 weeks in this patient. Therefore, *in vitro* experiments were conducted to characterize these treatments' potential mechanisms.

Materials and methods

Subject

This study on the collection of patient information was approved by the Research Ethics Committee of China Medical University & Hospital, Taichung, Taiwan [Identification No.: CMUH108-REC2-080] in accordance with the Declaration of Helsinki. The patient had signed the informed consent. The patient's clinical data were obtained from chart reviews and NGS results.

Cell lines and cell culture

The human pharyngeal squamous cell carcinoma cell line, FaDu, was bought from the American Type Culture Collection (ATCC). The human oral squamous carcinoma cell line, OECM-1, was bought from Sigma-Aldrich. FaDu cells were maintained in DMEM media (Invitrogen). OECM-1 cells were maintained in RPMI 1640 media (Invitrogen) supplemented with 2 mM L-glutamine. Both cell lines were grown in a humidified atmosphere of 5% CO_2 and 95% air at 37°C.

Chemical reagents

Asadin (arsenic trioxide, ATO) was bought from TTY Biopharm. Osimertinib (AZD9291, AZD) was bought from Cayman. 3-(4,5-dimethylthiazol-2-yl)-2,5-diphenyltetrazolium bromide (MTT; Cat. #M6494) and CM-H2DCFDA (Cat. #C6827) were bought from Invitrogen. Sequencing grade modified Trypsin (Cat. #V5111) was bought from Promega. Propidium iodide (PI; Cat. #P4170), acetonitrile (Cat. #34851), trifluoroacetic acid (Cat. #302031), and ammonia bicarbonate (Cat. # A6141) were purchased from Sigma-Aldrich.

In silica analysis

Pair-wise gene expression correlation analysis was conducted on the Gene Expression Profiling Interactive Analysis (GEPIA) web server (http://gepia.cancer-pku.cn/) using The Cancer Genome Atlas (TCGA) and Genotype-Tissue Expression (GTEx) expression data using a standard processing pipeline. The monotonic relationship between BRCA1 and PLK1 expression was calculated using the Spearman correlation coefficient.

Proteomic analysis

Proteomic alterations in FaDu cells untreated or treated with ATO (1 μM) or AZD (2.5 μM) alone or combined with ATO and AZD (1 μM/2.5 μM; ATO/AZD) were identified using mass spectrometric analysis (MS). Total proteins were extracted using RIPA lysis and extraction buffer (Thermo Fisher). Protein concentrations were determined using Bio-Rad Protein Assay kits by measuring absorbance at 595 nm. Each protein sample (40 μg) was electrophoresed using 9.5% SDS-PAGE and divided into five gel fractions. After fine cutting, an in-gel digestion procedure was used to generate tryptic peptides. The Orbitrap Exploris 480 mass spectrometer (Thermo Fisher Scientific) coupled with an Ultimate 3000 RSLC nanosystem (Thermo Fisher Scientific) was used for MS analysis. The MS instrument was operated in a positive ion mode with a data-dependent acquisition setting. Top N multiply charged precursors were automatically isolated and fragmented dependent on MS intensities within three seconds of cycle time. Full MS scan was set at a resolution of 120,000 with an automatic gain control target of 300%, and MS/MS scan was performed in the Orbitrap at a resolution of 30,000. Protein identification was conducted using Proteome Discoverer software v.2.4 (Thermo Fisher Scientific) with the SEQUEST HT search engine at a 1% false discovery rate. Labeling-free quantitation was conducted using the functional node of the Precursors Ions Quantifier.

Cell viability assay

The effects of ATO and AZD on cell viability were determined using the methylthiazol tetrazolium (MTT) technique. Tumor cells were seeded in 24-well microplates at a density of 2×10^4 cells/per well and treated using ATO (1 μM) or AZD (2.5 μM) for 24 hours. After treatment, 200 μL MTT solution (1 mg/mL in PBS) was added for 4 hours at 37°C. After eliminating the solution, 500 μL DMSO was used to dissolve insoluble purple formazan dyes. Cell viability was calculated using an optical density (OD) at a wavelength of 570 nm. The viability rate was defined as: cell viability (%) = (experiment OD570/control OD570) × 100%.

Intracellular ROS measurement

Trypsinized HNSCC cells (3×10^5 cells) were treated using 10 μM CM-H2DCFDA at 37°C for 30 minutes and then assessed using a BD FACSCalibur flow cytometer system and CellQuest software.

Comet assay

FaDu cells were untreated or treated with ATO (1 μM) or AZD (2.5 μM) alone or ATO/AZD (1 μM/2.5 μM) for 24 hours. FaDu cells (1×10^5/mL) were mixed with LMAgarose (#4250-050-02, CometAssay kit #, Trevigen) at a ratio of 1:10 (v/v) and placed onto the Trevigen CometSlide (#4250-050-03). The slides were then incubated in a cold Lysis Solution (#4250-050-01) for 1 hour. After the reaction with Alkaline Unwinding Solution (200 mM NaOH and 1 mM EDTA) for 20 minutes, the CometSlides were electrophoresed with freshly prepared cold Alkaline Electrophoresis Solution (200 mM NaOH and 1 mM EDTA, pH > 13) at 300 mA for 30 minutes. After electrophoresis, the CometSlides were washed using Neutral Electrophoresis Buffer and stained with SYBR Gold in the dark for 30 minutes. Images were obtained using a Leica TCS SP8 confocal microscope.

Western blotting

The total proteins were separated by 9.5% or 13% SDS-PAGE, dependent on the molecular weight of the target proteins. For Western blotting, proteins were transferred onto PVDF membranes at 400 mA at 0°C for 3 hours in 25 mM Tris-HCl, 197 mM glycine, and 13.3% (v/v) methanol. Membranes were blocked using 5% (w/v) skim milk in Tris-buffered saline with tween 20 (TBST) for 1 hour and then incubated with primary antibodies at 4°C for 16-18 hours. The primary antibodies used in this study

included BRCA1 (Cell Signaling, #9010), phospho-BRCA1 (Cell Signaling, #9009), PLK1 (Cell Signaling, #4513), γH2AX (Cell Signaling, #9718), and β-actin (Cell Signaling, #4970). After the membranes were washed for 15 min in TBST thrice, horseradish peroxidase-conjugated secondary antibodies were added, and the membranes were incubated at room temperature for 1 hour. After the same washing procedure, immunoreactive signals were shown using an enhanced ECL substrate Western Lighting Plus-ECL (PerkinElmer), and recorded using developing photographic film under optimum exposure conditions.

Immunofluorescence assay

For immunofluorescence assay, after culture media removal, HNSCC cells were washed with phosphate-buffered saline (PBS) and fixed with 4% paraformaldehyde for 10 minutes. Then, the tumor cells were permeabilized with 0.1% Triton X-100 for 5 minutes. After PBS washing, tumor cells were blocked using 1% bovine serum albumin (BSA) for 1 hours. Primary Rad51 antibody (Cell Signaling, #8875; 1:100 dilution) and secondary antibody AlexaFlour 488 (1:400 dilution) in PBS containing 1% BSA were used to react with tumor cells for 1 hours. Finally, tumor cells were treated using a DAPI mounting solution. The borders of the coverslips were sealed using nail polish. Fluorescence signals were found using a Leica TCS SP8 confocal microscope.

Statistical analyses

Data were displayed as the means ± SD. The significance of differences was examined by Student's *t*-test. *p*-values < 0.05 were considered statistically significant.

Results

Case presentation, an unusual response to ATO and AZD

A 41-year-old man was diagnosed with right oropharyngeal squamous cell carcinoma in advanced cT3N2bM0, Jul/2019. The treatment processes during Jul/2019-Apr/2021 are shown in **Figure 1A**. He received induction chemotherapy with TPF four times from Jul/2019 to Sep/2019. An initial response to induction chemotherapy was held for two months, after which the disease progressed with neck lymph node enlargement. The combined positive score (CPS), defined as the number of programmed cell death-ligand 1 (PD-L1) positive cells (tumor cells, lymphocytes, and macrophages) divided by the total number of tumor cells × 100, is used to select patients for pembrolizumab monotherapy. Due to CPS < 1 in this patient, the combination of pembrolizumab plus cetuximab and radiotherapy was administered since Oct/2019. After radiotherapy in Feb/2020, the therapeutic response was evaluated using a head and neck computed tomography (CT) scan, which exhibited a partial response. Therefore, the combination of pembrolizumab and cetuximab was continuously used for disease control. However, the following head and neck CT scan showed disease progression in Apr/2020. The treatment agents were shifted to the combination of nivolumab and ipilimumab, but the disease continued progressing from May/2020 to Jun/2020. The next genomic sequencing analysis showed a mutation of *TP53* and *BRCA2* genes in the patient's tumors (Table S1); thus, the patient received olaparib monotherapy since Jun/2020. The disease progression was noted again in Aug/2020. He then received a combination of pembrolizumab and lenvatinib from Sep/2020 to Oct/2020, but the disease kept progressing. Because of *TP53* mutation and EGFR overexpression, we suggested a genetics-guided treatment strategy as ATO 6 mg/m^2 plus AZD 80 mg daily since Oct/2020. A treatment cycle of ATO was set as two weeks off after two weeks of drug use. The facial pain and headache improved after 4 weeks of treatment. The first therapeutic evaluation showed a partial response on Dec/2020 (**Figure 1B**). The response lasted until Apr/2021, and the duration time of response to this treatment lasted for 24 weeks in this patient. For a patient with R/M HNSCC who is primary refractory to many treatments including cisplatin, cetuximab, immune checkpoint inhibitors, and radiotherapy, this is an unusual clinical response to this encouraging medication. Therefore, the unique regimen ATO/AZD may be developed as a novel therapeutic strategy for R/M HNSCC.

The combination of ATO and AZD exhibits a synergistic inhibitory effect on HNSCC

On the basis of the clinical observation, the combined treatment with ATO and AZD (ATO/AZD) could be conferred as a therapeutic ben-

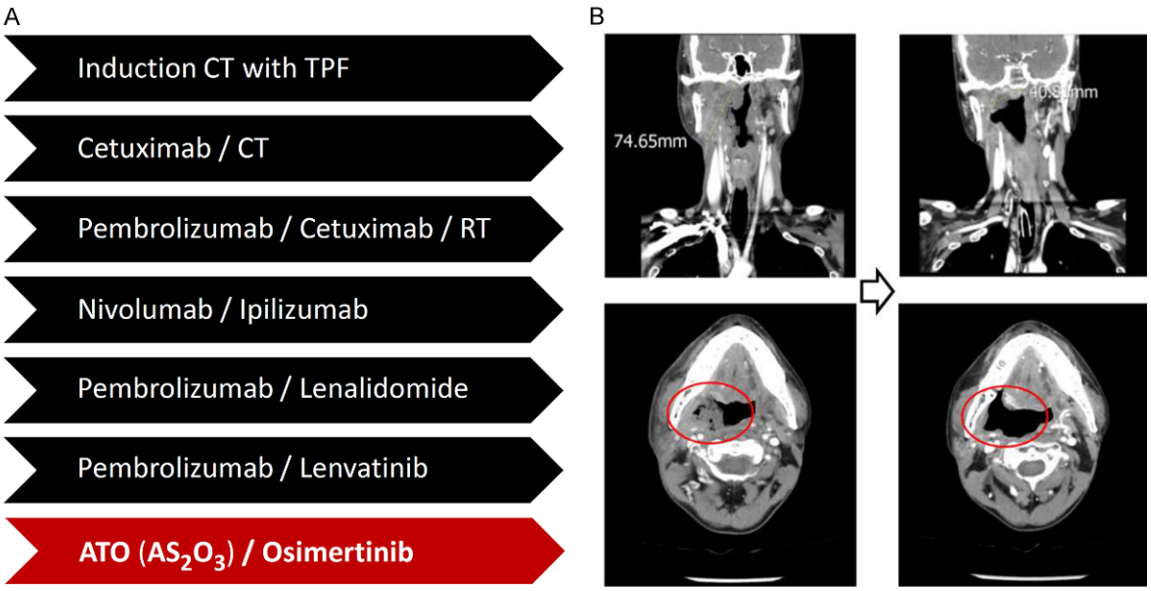

Figure 1. Patient treatment and the therapeutic assessment. A. The treatment processes of the patient from Jul/2019 to Apr/2021. B. The therapeutic evaluation of computed tomography in the patient before and after four weeks of ATO and AZD treatment.

efit to patients with R/M HNSCC for disease control. Thus, the impact of both agents on the cell survival of HNSCC tumor cells was determined by a combination index (CI). To this end, we first tested the FaDu cell line (human hypopharyngeal squamous cell carcinoma cell harboring *TP53* missense mutation at codon 248) with single-agent treatment. Cell viability MTT assay showed that the IC50 doses were 12 μM and 4.5 μM for ATO and AZD after 24 hr treatment, respectively (**Figure 2A** and **2B**). To study the synergistic effect of ATO and AZD on FaDu cells (and OECM-1 cells, results shown in Figure S1), we determined the inhibition rates of various drug concentrations of ATO or AZD alone and ATO/AZD. ATO/AZD treatment exhibited 75% effective dose (ED75) and ED90 values of 0.74 and 0.55, respectively, showing a synergistic inhibitory effect on cell growth of FaDu cells (**Figure 2C**).

ATO/AZD induce DNA damage in HNSCC

To explore the mechanisms underlying ATO/AZD treatment, quantitative proteomic analyses were performed to identify the changes in protein signature responding to the treatments of ATO or AZD alone or ATO/AZD in FaDu cells. Seven thousand one hundred and twenty-nine proteins were found in these analyses (Table S2). Proteomic changes in FaDu cells in each treatment are drawn in three-dimensional scatter plots, which display the relationship between ratio weights (weighting by mass intensity) and abundance ratios of each protein. The color of protein dots represents adjusted *p*-values for abundance ratios from the background T test (**Figure 3A-C**). ATO/AZD had a dominant effect on inhibiting protein expression (**Figure 3C**). Heat-map clustering analysis of significantly altered proteins with a *p*-value of abundance ratio < 0.05 showed alterations of their protein levels in response to different treatments (**Figure 3D**). The analytical results showed that these significantly altered proteins were most affected by AZD alone compared with ATO alone and a combination of ATO/AZD. Notably, the biological function search shows that among significantly altered proteins, 38.6% of upregulated (17 of 44) and 25.5% of downregulated (49 of 192) proteins are involved in the DNA damage and repair pathways (**Table 1**). This result is consistent with the previously reported findings that ATO and AZD were associated with induction of DNA damage [27, 28]. Excessive reactive oxygen species (ROS) cause oxidative stress and oxidative DNA damage [29]. ATO and AZD significantly increased intracellular ROS levels in HNSCC, particularly ATO/AZD treatment (**Figure 3E**). Consistently, Western blotting showed that

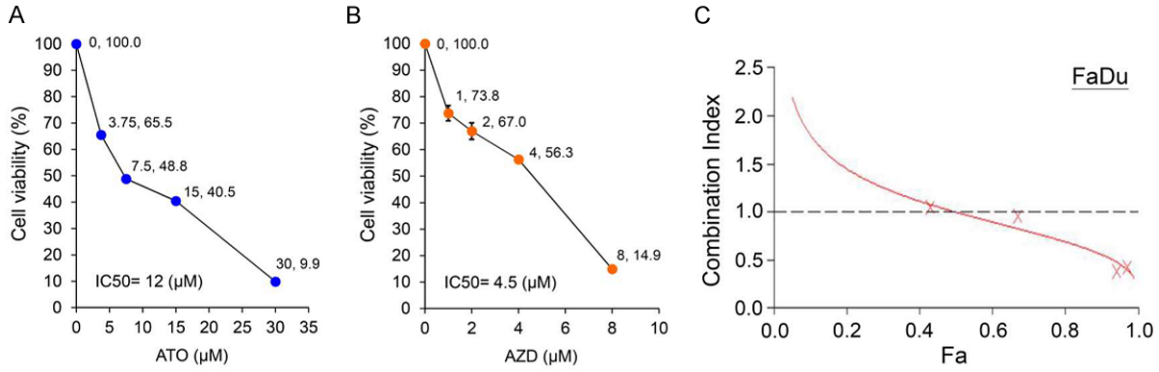

Figure 2. Combination index (CI) of combinatorial treatment with ATO and AZD. A. Dose-effect curve of ATO for FaDu cells. B. Dose-effect curve of AZD for FaDu cells. C. Fa-CI plot for FaDu cells.

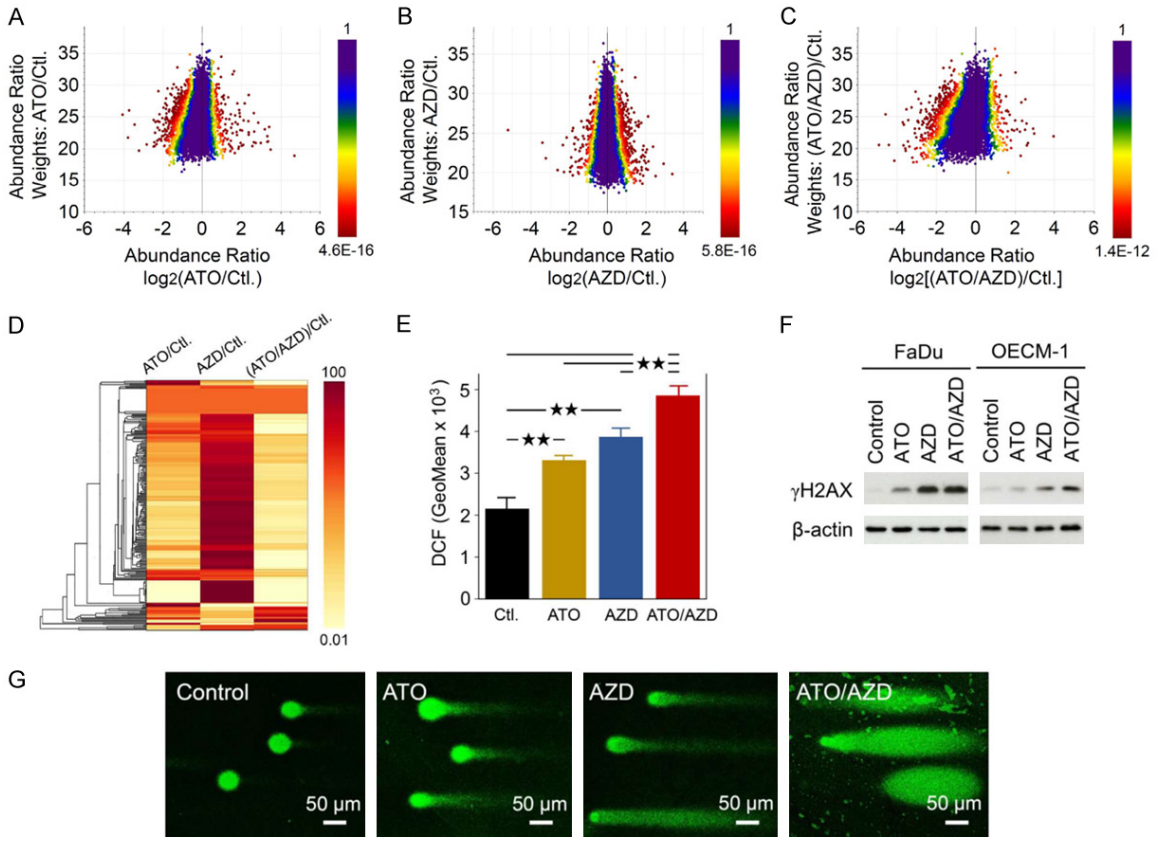

Figure 3. ATO/AZD induce DNA damage in HNSCC. Three-dimensional scatter plots showing the relationship between ratio weights and abundance ratios for each identified protein in the comparative proteomic analyses of (A) ATO vs. control, (B) AZD vs. control, and (C) ATO/AZD vs. control. The color of protein dots represent the *p*-value for corresponding abundance ratios. (D) Heat-map clustering analysis of quantified proteins with significant abundance ratios ($P < 0.05$) in the three comparative proteomes. (E) Intracellular ROS levels in FaDu cells untreated or treated with ATO or AZD alone or ATO/AZD were determined using the tracer dye, DCF, through flow cytometry. **, $P < 0.01$. (F) The γH2AX levels in FaDu and OECM-1 cells untreated or treated with ATO or AZD alone or ATO/AZD were determined using Western blotting. β-actin, loading control. (G) DNA damage in FaDu cells untreated or treated with ATO or AZD alone or ATO/AZD for 24 hours was determined using alkaline comet assay.

ATO/AZD markedly induced the expression of γH2AX, a well-known marker for DNA double-strand breaks [30], compared with ATO or AZD alone or untreated control (**Figure 3F**). In line

Table 1. The significantly altered proteins involved in DNA damage or repair pathways

A. Up-expressed protein in response to ATO/AZD			
Gene name	Protein name	Gene name	Abundance Ratio (ATO/AZD)/Ctl.
HMOX1	Heme oxygenase 1	HMOX1	100
SMARCA1	Probable global transcription activator SNF2L1	SMARCA1	100
MT1E	Metallothionein-1E	MT1E	100
UBE2E3	Ubiquitin-conjugating enzyme E2 E3	UBE2E3	100
RIT1	GTP-binding protein Rit1	RIT1	100
PCSK9	Proprotein convertase subtilisin/kexin type 9	PCSK9	100
PINX1	PIN2/TERF1-interacting telomerase inhibitor 1	PINX1	100
CEBPD	CCAAT/enhancer-binding protein delta	CEBPD	100
TP73	Tumor protein p73	TP73	100
PDK1	[Pyruvate dehydrogenase (acetyl-transferring)] kinase isozyme 1, mitochondrial	PDK1	7.86
VIM	Vimentin	VIM	5.99
AKR1C3	Aldo-keto reductase family 1 member C3	AKR1C3	5.72
GDF15	Growth/differentiation factor 15	GDF15	5.16
AKT3	RAC-gamma serine/threonine-protein kinase	AKT3	4.75
LCN2	Neutrophil gelatinase-associated lipocalin	LCN2	4.30
ANXA1	Annexin A1	ANXA1	4.11
PDCD4	Programmed cell death protein 4	PDCD4	3.04
B. Down-expressed protein in response to ATO/AZD			
Gene name	Protein name	Gene name	Abundance Ratio (ATO/AZD)/Ctl.
AHNAK	Neuroblast differentiation-associated protein AHNAK	AHNAK	0.40
DNMT1	DNA (cytosine-5)-methyltransferase 1	DNMT1	0.40
SNRNP200	U5 small nuclear ribonucleoprotein 200 kDa helicase	SNRNP200	0.39
RCC2	Protein RCC2	RCC2	0.36
FANCI	Fanconi anemia group I protein	FANCI	0.35
CHD4	Chromodomain-helicase-DNA-binding protein 4	CHD4	0.35
DHX9	ATP-dependent RNA helicase A	DHX9	0.33
DDX21	Nucleolar RNA helicase 2	DDX21	0.33
RECQL	ATP-dependent DNA helicase Q1	RECQL	0.32
ANT2	ADP/ATP translocase 2	ANT2	0.32
TRRAP	Transformation/transcription domain-associated protein	TRRAP	0.32
EP300	Histone acetyltransferase p300	EP300	0.32
MSH6	DNA mismatch repair protein Msh6	MSH6	0.31
MCM5	DNA replication licensing factor MCM5	MCM5	0.28
PRMT1	Protein arginine N-methyltransferase 1	PRMT1	0.28
CEP131	Centrosomal protein of 131 kDa	CEP131	0.27
USP24	Ubiquitin carboxyl-terminal hydrolase 24	USP24	0.26
PML	Protein PML	PML	0.26
NAT10	RNA cytidine acetyltransferase	NAT10	0.25
PLK1	Serine/threonine-protein kinase PLK1	PLK1	0.24
CHD3	Chromodomain-helicase-DNA-binding protein 3	CHD3	0.22
PKMYT1	Membrane-associated tyrosine- and threonine-specific cdc2-inhibitory kinase	PKMYT1	0.22
SETDB1	Histone-lysine N-methyltransferase SETDB1	SETDB1	0.22
DICER1	Endoribonuclease Dicer	DICER1	0.21
ERCC6	DNA excision repair protein ERCC-6	ERCC6	0.21
HERC2	E3 ubiquitin-protein ligase HERC2	HERC2	0.21
RRM2	Ribonucleoside-diphosphate reductase subunit M2	RRM2	0.20
TSC2	Tuberin	TSC2	0.20

TMBIM6	Bax inhibitor 1	TMBIM6	0.20
WDR18	WD repeat-containing protein 18	WDR18	0.18
EP400	E1A-binding protein p400	EP400	0.18
ATR	Serine/threonine-protein kinase ATR	ATR	0.17
SETX	Probable helicase senataxin	SETX	0.15
POLE	DNA polymerase epsilon catalytic subunit A	POLE	0.12
NSD2	Histone-lysine N-methyltransferase NSD2	NSD2	0.09
SLC35F2	Solute carrier family 35 member F2	SLC35F2	0.09
TXNL1	Thioredoxin-like protein 1	TXNL1	0.09
APOBEC3F	DNA dC->dU-editing enzyme APOBEC-3F	APOBEC3F	0.09
INO80	Chromatin-remodeling ATPase INO80	INO80	0.08
FLI1	Friend leukemia integration 1 transcription factor	FLI1	0.01
RAF1	RAF proto-oncogene serine/threonine-protein kinase	RAF1	0.01
CCNC	Cyclin-C	CCNC	0.01
ARNTL	Aryl hydrocarbon receptor nuclear translocator-like protein 1	ARNTL	0.01
RAD54L	DNA repair and recombination protein RAD54-like	RAD54L	0.01
CDT1	DNA replication factor Cdt1	CDT1	0.01
NEIL2	Endonuclease 8-like 2	NEIL2	0.01
LYZ	Lysozyme C	LYZ	0.01
PRDM16	Histone-lysine N-methyltransferase PRDM16	PRDM16	0.01
ZNHIT1	Zinc finger HIT domain-containing protein 1	ZNHIT1	0.01

with the Western blotting finding, ATO/AZD caused more scattered DNA tailing than ATO or AZD treatment alone in the comet assay (**Figure 3G**).

ATO/AZD impairs DNA damage repair response via suppression of BRCA1-PLK1 signaling

Previous reports suggested that ATO and AZD could delay DNA damage repair [27, 28], thus it is speculated that a marked increase in DNA damage by ATO/AZD might be from attenuating the DNA damage repair response. In response to DNA damage, RAD51 assembles as a nucleoprotein filament around DNA to promote homology recognition for the repair of DNA double-strand breaks [31]. Confocal microscopy showed that ATO/AZD reduced the formation of nuclear Rad51 foci in HNSCC cells compared with each alone (**Figure 4A**), implicating ATO/AZD may impair recruitment of Rad51 to DNA double-strand lesions for repair. On the basis of our proteomic findings (**Figure 4B** and **Table 1**), ATO/AZD inhibited the expression of polo-like kinase 1 (PLK1), which could be responsible for the RAD51 recruitment through the phosphorylation of RAD51 at serine 14 [32]. The suppression of PLK1 upon ATO/AZD treatment was validated by Western blotting (**Figure 4C**). In consistent with the expression of PLK1 during late G2 and M phases, ATO/AZD primarily caused G2/M phase cell cycle arrest (**Figure 4D**). Recent studies showed that the breast cancer type 1 susceptibility protein (BRCA1) plays an important role in controlling PLK1 activity to correctly orient the cell division in breast cancer [33]. It was found that ATO/AZD also inhibited BRCA1 expression in the proteomic analysis (**Figure 4B**). Western blotting showed that ATO/AZD decreases the BRCA1 levels and the phosphorylated form of BRCA1 to inhibit its activity (**Figure 4C**). Additionally, a significantly positive correlation between BRCA1 and PLK1 expression in HNSCC was found by *in silica* gene expression analysis using the TCGA RNA-Seq database (**Figure 4E**). Altogether, these results suggest that ATO/AZD could attenuate the BRCA1-PLK1 signaling pathway, thereby impairing DNA damage repair response in HNSCC.

Discussion

In this study, we present a patient with R/M HNSCC who was primarily resistant to platinum chemotherapy, checkpoint inhibitors, and cetuximab plus chemotherapy and attained a durable response to a genetics-guided combinatorial ATO/AZD treatment. The first-line treatment of R/M HNSCC had shifted to checkpoint inhibitors pembrolizumab plus PF or pembroli-

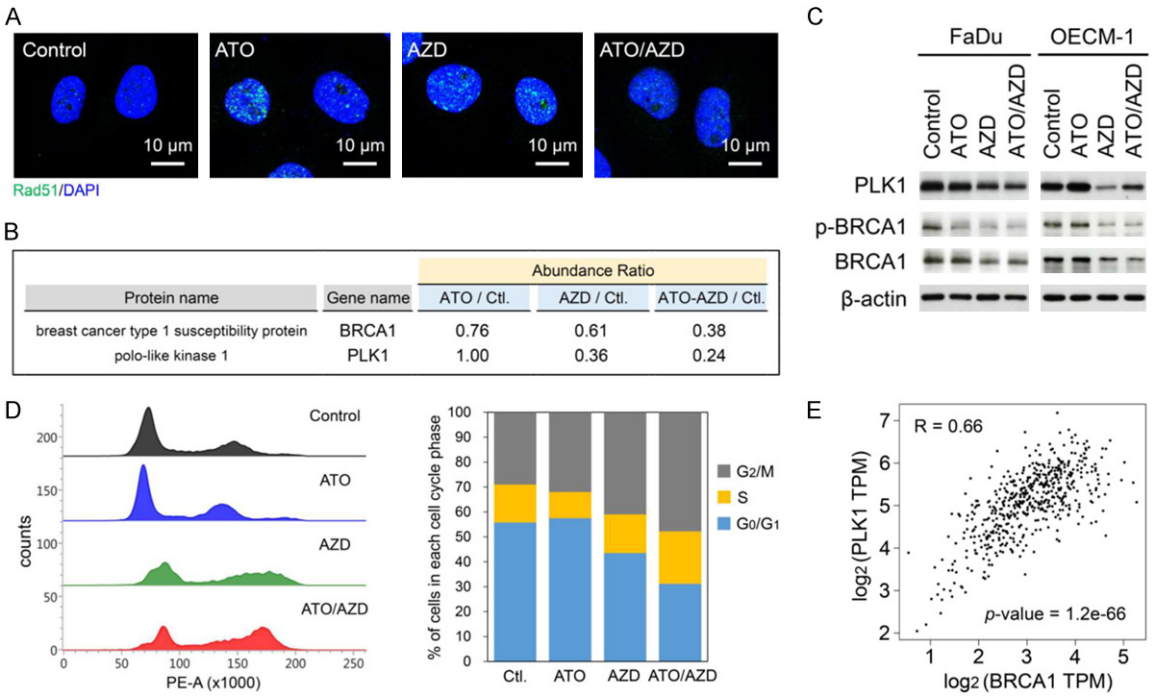

Figure 4. ATO/AZD impairs the DNA damage repair response by reducing RAD51 recruitment. A. Nuclear Rad51 foci in OECM-1 cells untreated or treated with ATO or AZD alone or ATO/AZD for four hours were evaluated using fluorescence microscopy. Green, RAD51; Blue, nucleus. B. Change in the BRCA1 and PLK1 levels in the comparative proteomic analyses of FaDu cells. The abundance ratio was normalized by the control group. C. PLK1, BRCA1, and phosphor-BRCA1 levels in FaDu and OECM-1 cells untreated or treated with ATO or AZD alone or ATO/AZD for 24 hours were determined using Western blotting. β-actin, loading control. D. After serum starvation for synchronization, FaDu cells were untreated or treated with ATO or AZD alone or ATO/AZD for 24 hours. DNA content in each cell cycle phase was measured using propidium iodide staining. Data are presented as representative histograms (left part) and bar graphs (right part). E. Spearman's monotonic correlation between BRCA1 and PLK1 expression in HNSCC was evaluated using the TCGA RNA-Seq database on the GEPIA web server.

zumab alone when CPS > 20 currently [34]. However, an ORR to pembrolizumab and a PFS in patients with HNSCC remain frustrating. Approximately 20% of patients showed long-term survival benefits, but the remainder of patients progressed rapidly [9]. After progression from an anti-PD-1 agent, there is no standard treatment for these patients. Before checkpoint inhibitors got FDA approval, cetuximab combined with chemotherapy was the most successful treatment for R/M HNSCC. Clinically, cetuximab shows a response rate of 13% and a median progression-free survival of 2.3 months [16, 35]. Cetuximab combined with PF in platinum-sensitive HNSCC patients increased an ORR to 36% and prolonged PFS to 5.6 months compared with chemotherapy alone in the EXTRME trial [36]. Tyrosine kinase inhibitor (TKI) is another strategy to target EGFR, which is frequently overexpressed in HNSCC tumors [14]. For instance, afatinib has been approved for use in NSCLC with EGFR mutation. Unfortunately, EGFR-TKI has shown to have limited clinical efficacy with response rates of 10%-15% and no benefit in OS for HNSCC patients [37], implicating the necessity for EGFR-TKI combination treatment to overcome resistance and increase therapeutic efficacy. In our reported case, the third-generation EGFR-TKI osimertinib (AZD) was recommended for therapeutic consideration because of the lower incidence of severe rash and diarrhea than afatinib.

ATO, a first-line therapeutic agent for APL, directly binds with promyelocytic leukemia-retinoic acid receptor α and enhances the product degradation through the ubiquitin-proteasome system, thereby promoting the differentiation of APL cells [38]. Although single-agent ATO exhibits promising results in different types of solid tumors, including esophageal, gastric,

hepatic, ovarian, pancreatic, and prostatic carcinomas *in vitro* and *in vivo* [39]; however, no significant therapeutic ATO efficacy has been demonstrated in clinical trials yet [40]. A relatively high doses of ATO is required to treat solid tumors than APL, potentially causing a serious limitation on the clinical use of ATO because of severe adverse events, including cardiotoxicity, hepatotoxicity, and nephrotoxicity. Therefore, the ATO combination for decreasing dose-derived toxicities has emerged as an alternative treatment strategy for solid tumors. Besides directly targeting tumors, ATO shows capabilities of immunomodulation to activate T-cells and regulate macrophage polarization in the tumor microenvironment [41, 42]. Our recent study demonstrated that ATO sensitizes HNSCC to docetaxel by minimizing macrophage infiltration and impairing IL-1β secretion by macrophages [43], providing an optimal ATO combination for cancer treatment. In patients with HNSCC, frequent genetic alterations and gene enrichments are found in *TP53*, *CDKN2A*, *CASP8*, *FAT1*, *NOTCH1*, *HRAS*, *PIK3CA*, *MLL2*, and *FBXW7* [22]. The gain-of-function *TP53* mutations exhibit many oncogenic features, including causing genomic instability, epithelial-to-mesenchymal transition, inflammation, and metabolic reprogramming in tumor cells [23]. Recently, ATO stabilizes structural p53 mutants thereby restoring the wild-type functions of p53 [26], implicating the possible roles of ATO in HNSCC therapy.

Combination index analyses revealed a synergistic inhibitory effect on HNSCC cells by ATO/AZD (**Figure 2C** and Figure S1). ATO and AZD increase intracellular ROS levels, thereby inducing DNA damage [27, 44], which is consistent with our validation (**Figure 3E**). In line with this result, it was observed that ATO and AZD increase γH2AX accumulation, particularly in ATO/AZD combination (**Figure 3F**). Additionally, EGFR and the tumor suppressor p53 have been identified to play essential roles in DNA repair mechanisms [45, 46]. In response to DNA damage stress EGFR can translocate to the nucleus to interact with DNA repair proteins and regulate DNA repair [46, 47]. The activity of p53 has been associated with the inhibition of RAD51-mediated homologous recombination (HR) DNA repair [48]. Indeed, ATO/AZD markedly decreased the formation of nuclear RAD51 foci (**Figure 4A**) and caused G2/M phase cell cycle arrest (**Figure 4D**). On the basis of the proteomic findings, ATO/AZD attenuates DNA repair likely through inhibiting BRCA1 and the downstream effector PLK1 [33] to reduce RAD51-mediated HR DNA repair (**Figure 4C**), thereby inhibiting tumor growth and causing tumor death.

In conclusion, both genetic clues, EGFR overexpression and p53 mutation, rendered us to suggest an ATO/AZD combination for the heavily treated HNSCC patient, who finally received treatment response and PFS for about six months. ATO/AZD causes significant DNA damage and impairs the DNA damage response for DNA repair, which provides strong mechanical support for this combinatorial treatment. Although the finding in a single-case hardly leads to a definite conclusion, this study at least provides an encouraging experience of ATO/AZD therapy for R/M HNSCC and suggests that it is worthy of consideration for further clinical trials to improve therapeutic efficacy.

Acknowledgements

We thank the Proteomics Core Facility of the Research Center for Cancer Biology, China Medical University, Taichung 40402, Taiwan. This study was supported by the National Health Research Institutes (NHRI-180A1-CACO-13191902) and the National Science and Technology Council (NSTC, Grant No. 111-2320-B-039-029-MY2, 111-2314-B-039-033-MY3, 111-2639-B-039-001-ASP) and China Medical University Hospital (Grant No. DMR-111-009), Taiwan.

Disclosure of conflict of interest

None.

Address correspondence to: Mien-Chie Hung, College of Medicine, Graduate Institute of Biomedical Sciences, China Medical University, Taichung 40402, Taiwan. E-mail: mhung@cmu.edu.tw; Wei-Chao Chang, Center for Molecular Medicine, China Medical University Hospital, China Medical University, Taichung 40402, Taiwan. E-mail: t21443@mail.cmuh.org.tw

References

[1] Bray F, Ferlay J, Soerjomataram I, Siegel RL, Torre LA and Jemal A. Global cancer statistics 2018: GLOBOCAN estimates of incidence and

mortality worldwide for 36 cancers in 185 countries. CA Cancer J Clin 2018; 68: 394-424.
[2] Johnson DE, Burtness B, Leemans CR, Lui VWY, Bauman JE and Grandis JR. Head and neck squamous cell carcinoma. Nat Rev Dis Primers 2020; 6: 92.
[3] D'Cruz AK, Vaish R, Kapre N, Dandekar M, Gupta S, Hawaldar R, Agarwal JP, Pantvaidya G, Chaukar D, Deshmukh A, Kane S, Arya S, Ghosh-Laskar S, Chaturvedi P, Pai P, Nair S, Nair D and Badwe R; Head and Neck Disease Management Group. Elective versus therapeutic neck dissection in node-negative oral cancer. N Engl J Med 2015; 373: 521-529.
[4] Chow LQM. Head and neck cancer. N Engl J Med 2020; 382: 60-72.
[5] Parmar A, Macluskey M, Mc Goldrick N, Conway DI, Glenny AM, Clarkson JE, Worthington HV and Chan KK. Interventions for the treatment of oral cavity and oropharyngeal cancer: chemotherapy. Cochrane Database Syst Rev 2021; 12: CD006386.
[6] Kim KR, Shim HJ, Hwang JE, Cho SH, Chung IJ, Park KS, Kang SR, Kwon SY, Chung WK and Bae WK. The role of interim FDG PET-CT after induction chemotherapy as a predictor of concurrent chemoradiotherapy efficacy and prognosis for head and neck cancer. Eur J Nucl Med Mol Imaging 2018; 45: 170-178.
[7] Hsieh CY, Lein MY, Yang SN, Wang YC, Lin YJ, Lin CY, Hua CH, Tsai MH and Lin CC. Dose-dense TPF induction chemotherapy for locally advanced head and neck cancer: a phase II study. BMC Cancer 2020; 20: 832.
[8] Bonner JA, Harari PM, Giralt J, Azarnia N, Shin DM, Cohen RB, Jones CU, Sur R, Raben D, Jassem J, Ove R, Kies MS, Baselga J, Youssoufian H, Amellal N, Rowinsky EK and Ang KK. Radiotherapy plus cetuximab for squamous-cell carcinoma of the head and neck. N Engl J Med 2006; 354: 567-578.
[9] Seiwert TY, Burtness B, Mehra R, Weiss J, Berger R, Eder JP, Heath K, McClanahan T, Lunceford J, Gause C, Cheng JD and Chow LQ. Safety and clinical activity of pembrolizumab for treatment of recurrent or metastatic squamous cell carcinoma of the head and neck (KEYNOTE-012): an open-label, multicentre, phase 1b trial. Lancet Oncol 2016; 17: 956-965.
[10] Ferris RL, Blumenschein G Jr, Fayette J, Guigay J, Colevas AD, Licitra L, Harrington K, Kasper S, Vokes EE, Even C, Worden F, Saba NF, Iglesias Docampo LC, Haddad R, Rordorf T, Kiyota N, Tahara M, Monga M, Lynch M, Geese WJ, Kopit J, Shaw JW and Gillison ML. Nivolumab for recurrent squamous-cell carcinoma of the head and neck. N Engl J Med 2016; 375: 1856-1867.
[11] Burtness B, Harrington KJ, Greil R, Soulières D, Tahara M, de Castro G Jr, Psyrri A, Basté N, Neupane P, Bratland Å, Fuereder T, Hughes BGM, Mesía R, Ngamphaiboon N, Rordorf T, Wan Ishak WZ, Hong RL, González Mendoza R, Roy A, Zhang Y, Gumuscu B, Cheng JD, Jin F and Rischin D; KEYNOTE-048 Investigators. Pembrolizumab alone or with chemotherapy versus cetuximab with chemotherapy for recurrent or metastatic squamous cell carcinoma of the head and neck (KEYNOTE-048): a randomised, open-label, phase 3 study. Lancet 2019; 394: 1915-1928.
[12] Califano J, van der Riet P, Westra W, Nawroz H, Clayman G, Piantadosi S, Corio R, Lee D, Greenberg B, Koch W and Sidransky D. Genetic progression model for head and neck cancer: implications for field cancerization. Cancer Res 1996; 56: 2488-2492.
[13] Tsimberidou AM, Wen S, Hong DS, Wheler JJ, Falchook GS, Fu S, Piha-Paul S, Naing A, Janku F, Aldape K, Ye Y, Kurzrock R and Berry D. Personalized medicine for patients with advanced cancer in the phase I program at MD Anderson: validation and landmark analyses. Clin Cancer Res 2014; 20: 4827-4836.
[14] Kalyankrishna S and Grandis JR. Epidermal growth factor receptor biology in head and neck cancer. J Clin Oncol 2006; 24: 2666-2672.
[15] Zhu X, Zhang F, Zhang W, He J, Zhao Y and Chen X. Prognostic role of epidermal growth factor receptor in head and neck cancer: a meta-analysis. J Surg Oncol 2013; 108: 387-397.
[16] Colevas AD. Chemotherapy options for patients with metastatic or recurrent squamous cell carcinoma of the head and neck. J Clin Oncol 2006; 24: 2644-2652.
[17] Liao HW, Hsu JM, Xia W, Wang HL, Wang YN, Chang WC, Arold ST, Chou CK, Tsou PH, Yamaguchi H, Fang YF, Lee HJ, Lee HH, Tai SK, Yang MH, Morelli MP, Sen M, Ladbury JE, Chen CH, Grandis JR, Kopetz S and Hung MC. PRMT1-mediated methylation of the EGF receptor regulates signaling and cetuximab response. J Clin Invest 2015; 125: 4529-4543.
[18] Wang WJ, Hsu JM, Wang YN, Lee HH, Yamaguchi H, Liao HW and Hung MC. An essential role of PRMT1-mediated EGFR methylation in EGFR activation by ribonuclease 5. Am J Cancer Res 2019; 9: 180-185.
[19] Madoz-Gúrpide J, Zazo S, Chamizo C, Casado V, Caramés C, Gavín E, Cristóbal I, García-Foncillas J and Rojo F. Activation of MET pathway predicts poor outcome to cetuximab in pa-

tients with recurrent or metastatic head and neck cancer. J Transl Med 2015; 13: 282.
[20] Alsahafi E, Begg K, Amelio I, Raulf N, Lucarelli P, Sauter T and Tavassoli M. Clinical update on head and neck cancer: molecular biology and ongoing challenges. Cell Death Dis 2019; 10: 540.
[21] Sullivan KD, Galbraith MD, Andrysik Z and Espinosa JM. Mechanisms of transcriptional regulation by p53. Cell Death Differ 2018; 25: 133-143.
[22] Cancer Genome Atlas Network. Comprehensive genomic characterization of head and neck squamous cell carcinomas. Nature 2015; 517: 576-582.
[23] Nathan CA, Khandelwal AR, Wolf GT, Rodrigo JP, Mäkitie AA, Saba NF, Forastiere AA, Bradford CR and Ferlito A. TP53 mutations in head and neck cancer. Mol Carcinog 2022; 61: 385-391.
[24] Zhou S, Fan C, Zeng Z, Young KH and Li Y. Clinical and immunological effects of p53-targeting vaccines. Front Cell Dev Biol 2021; 9: 762796.
[25] Xu J, Acharya S, Sahin O, Zhang Q, Saito Y, Yao J, Wang H, Li P, Zhang L, Lowery FJ, Kuo WL, Xiao Y, Ensor J, Sahin AA, Zhang XH, Hung MC, Zhang JD and Yu D. 14-3-3ζ turns TGF-β's function from tumor suppressor to metastasis promoter in breast cancer by contextual changes of Smad partners from p53 to Gli2. Cancer Cell 2015; 27: 177-192.
[26] Chen S, Wu JL, Liang Y, Tang YG, Song HX, Wu LL, Xing YF, Yan N, Li YT, Wang ZY, Xiao SJ, Lu X, Chen SJ and Lu M. Arsenic trioxide rescues structural p53 mutations through a cryptic allosteric site. Cancer Cell 2021; 39: 225-239, e8.
[27] Chayapong J, Madhyastha H, Madhyastha R, Nurrahmah QI, Nakajima Y, Choijookhuu N, Hishikawa Y and Maruyama M. Arsenic trioxide induces ROS activity and DNA damage, leading to G0/G1 extension in skin fibroblasts through the ATM-ATR-associated Chk pathway. Environ Sci Pollut Res Int 2017; 24: 5316-5325.
[28] Wu S, Zhu L, Tu L, Chen S, Huang H, Zhang J, Ma S and Zhang S. AZD9291 increases sensitivity to radiation in PC-9-IR cells by delaying DNA damage repair after irradiation and inducing apoptosis. Radiat Res 2018; 189: 283-291.
[29] AbdulSalam SF, Thowfeik FS and Merino EJ. Excessive reactive oxygen species and exotic DNA lesions as an exploitable liability. Biochemistry 2016; 55: 5341-5352.
[30] Ivashkevich A, Redon CE, Nakamura AJ, Martin RF and Martin OA. Use of the γ-H2AX assay to monitor DNA damage and repair in translational cancer research. Cancer Lett 2012; 327: 123-133.
[31] Wang Z, Jia R, Wang L, Yang Q, Hu X, Fu Q, Zhang X, Li W and Ren Y. The emerging roles of Rad51 in cancer and its potential as a therapeutic target. Front Oncol 2022; 12: 935593.
[32] Yata K, Lloyd J, Maslen S, Bleuyard JY, Skehel M, Smerdon SJ and Esashi F. Plk1 and CK2 act in concert to regulate Rad51 during DNA double strand break repair. Mol Cell 2012; 45: 371-383.
[33] He Z, Ghorayeb R, Tan S, Chen K, Lorentzian AC, Bottyan J, Aalam SMM, Pujana MA, Lange PF, Kannan N, Eaves CJ and Maxwell CA. Pathogenic BRCA1 variants disrupt PLK1-regulation of mitotic spindle orientation. Nat Commun 2022; 13: 2200.
[34] Burtness B, Rischin D, Greil R, Soulières D, Tahara M, de Castro G Jr, Psyrri A, Brana I, Basté N, Neupane P, Bratland Å, Fuereder T, Hughes BGM, Mesia R, Ngamphaiboon N, Rordorf T, Wan Ishak WZ, Ge J, Swaby RF, Gumuscu B and Harrington K. Pembrolizumab alone or with chemotherapy for recurrent/metastatic head and neck squamous cell carcinoma in KEYNOTE-048: subgroup analysis by programmed death ligand-1 combined positive score. J Clin Oncol 2022; 40: 2321-2332.
[35] Vermorken JB, Herbst RS, Leon X, Amellal N and Baselga J. Overview of the efficacy of cetuximab in recurrent and/or metastatic squamous cell carcinoma of the head and neck in patients who previously failed platinum-based therapies. Cancer 2008; 112: 2710-2719.
[36] Vermorken JB, Mesia R, Rivera F, Remenar E, Kawecki A, Rottey S, Erfan J, Zabolotnyy D, Kienzer HR, Cupissol D, Peyrade F, Benasso M, Vynnychenko I, De Raucourt D, Bokemeyer C, Schueler A, Amellal N and Hitt R. Platinum-based chemotherapy plus cetuximab in head and neck cancer. N Engl J Med 2008; 359: 1116-1127.
[37] Stewart JS, Cohen EE, Licitra L, Van Herpen CM, Khorprasert C, Soulieres D, Vodvarka P, Rischin D, Garin AM, Hirsch FR, Varella-Garcia M, Ghiorghiu S, Hargreaves L, Armour A, Speake G, Swaisland A and Vokes EE. Phase III study of gefitinib compared with intravenous methotrexate for recurrent squamous cell carcinoma of the head and neck. J Clin Oncol 2009; 27: 1864-1871.
[38] Lengfelder E, Hofmann WK and Nowak D. Impact of arsenic trioxide in the treatment of acute promyelocytic leukemia. Leukemia 2012; 26: 433-442.
[39] Wang QQ, Jiang Y and Naranmandura H. Therapeutic strategy of arsenic trioxide in the fight against cancers and other diseases. Metallomics 2020; 12: 326-336.

[40] Subbarayan PR and Ardalan B. In the war against solid tumors arsenic trioxide needs partners. J Gastrointest Cancer 2014; 45: 363-371.
[41] Gao Q, Jiang J, Chu Z, Lin H, Zhou X and Liang X. Arsenic trioxide inhibits tumor-induced myeloid-derived suppressor cells and enhances T-cell activity. Oncol Lett 2017; 13: 2141-2150.
[42] Liu X, Su Y, Sun X, Fu H, Huang Q, Chen Q, Mo X, Lv M, Kong Y, Xu L, Huang X and Zhang X. Arsenic trioxide alleviates acute graft-versus-host disease by modulating macrophage polarization. Sci China Life Sci 2020; 63: 1744-1754.
[43] Hsieh CY, Lin CC, Huang YW, Chen JH, Tsou YA, Chang LC, Fan CC, Lin CY and Chang WC. Macrophage secretory IL-1β promotes docetaxel resistance in head and neck squamous carcinoma via SOD2/CAT-ICAM1 signaling. JCI Insight 2022; [Epub ahead of print].
[44] Tang ZH, Cao WX, Su MX, Chen X and Lu JJ. Osimertinib induces autophagy and apoptosis via reactive oxygen species generation in non-small cell lung cancer cells. Toxicol Appl Pharmacol 2017; 321: 18-26.
[45] Zhang XP, Liu F and Wang W. Two-phase dynamics of p53 in the DNA damage response. Proc Natl Acad Sci U S A 2011; 108: 8990-8995.
[46] Liccardi G, Hartley JA and Hochhauser D. EGFR nuclear translocation modulates DNA repair following cisplatin and ionizing radiation treatment. Cancer Res 2011; 71: 1103-1114.
[47] Xie Y and Hung MC. Nuclear localization of p185neu tyrosine kinase and its association with transcriptional transactivation. Biochem Biophys Res Commun 1994; 203: 1589-1598.
[48] Smeby J, Kryeziu K, Berg KCG, Eilertsen IA, Eide PW, Johannessen B, Guren MG, Nesbakken A, Bruun J, Lothe RA and Sveen A. Molecular correlates of sensitivity to PARP inhibition beyond homologous recombination deficiency in pre-clinical models of colorectal cancer point to wild-type TP53 activity. EBioMedicine 2020; 59: 102923.

Table S1. Gene analysis of NGS in the patient

Gene	Alteration
VEGFA	amplification
CCND3	amplification
MYC	amplification-equivocal
ACVR1B	M1fs*47
BRCA2	K2570fs*78
TP53	E51fs*73

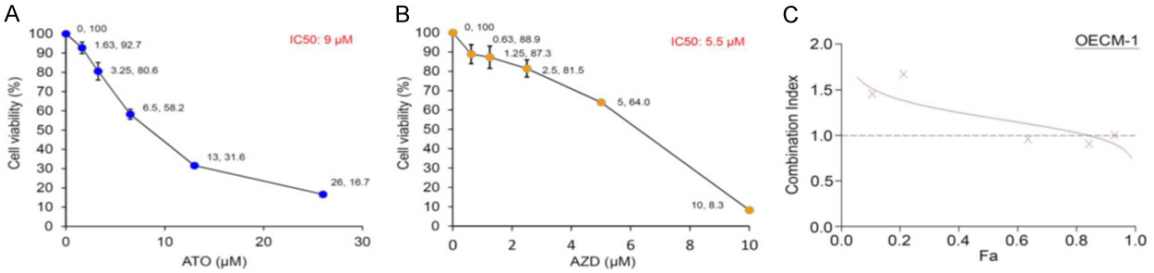

Figure S1. Combination index (CI) of combinatorial treatment with ATO and AZD. A. Dose-effect curve of ATO for OECM-1 cells. B. Dose-effect curve of AZD for OECM-1 cells. C. Fa-CI plot for OECM-1 cells.